Modelling of hydrostatic bearings for servo-cylinders

Barbara Zardin, Emiliano Natali, Giovanni Cillo, and Massimo Borghi

View Online   Export Citation

ARTICLES YOU MAY BE INTERESTED IN

AIP Conference Proceedings

Modelling of Hydrostatic Bearings For Servo-Cylinders

Barbara Zardin[a)], Emiliano Natali[b)], Giovanni Cillo[c)], Massimo Borghi[d)]

Fluid Power Lab, Engineering Department Enzo Ferrari, via P. Vivarelli 10, 41125 Modena, Italy.

[a)]barbara.zardin@unimore.it [b)]emiliano.natali@unimore.it [c)]giovanni.cillo@unimore.it [d)]massimo.borghi@unimore.it

Abstract. Hydraulic servo cylinders are widely used in versatile industrial applications such as machine tools, industrial robots, autonomous manufacturing systems and special applications in laboratories. To reduce friction and allow smooth and controllable displacement of the actuator, hydrostatic journal bearings are used at the ends of the rod. The design and manufacturing of this elements is challenging since the good operation relays on the very small tolerances required to bear the load on the cylinder and to reduce leakages. In this work, a virtual design and test tool for hydrostatic journal bearing with pockets, developed in OpenModelica environment, is presented. The influence of eccentricity and manufacturing tolerances is then studied and discussed. The model proposed has the aim to explore the extreme and critical operating conditions of the servo-cylinder and to help and/or improve the design phase.

INTRODUCTION

Lubricated interfaces in fluid power components are one of the most critical issues to be carefully designed for assessing a smooth behavior and good efficiencies in a system.

They are fundamental to analyze the complex phenomena determining the positive displacement pumps and motors efficiency, [1], and also fault behavior, see for example [2], where the slipper bearing worn condition is detected and analyzed as one of the main fault causes for pumps. As a consequence, many researchers in literature stated the necessity to introduce 2D or 3D fluid-dynamic analysis of the lubricated interfaces to assess the machine behavior ([3], [4], [5]) and the efficiency. Those efficiencies play an even more critical role on mobile applications, for example while addressing the operation of a hybrid vehicle as in [6]. Moreover, the issue of lubrication also affects the behavior of valves and linear actuators. Among the category of linear actuators, the servo cylinders are considered in this work, in particular the ones equipped with hydrostatic journal bearing with pockets at the rod ends and circumferential grooves on the piston surface.

Servo cylinders are typically used in test rigs for any kind of components/systems, in machine tools, in material testing devices and whenever a smooth movement with low friction, fast dynamic response and possible radial forces are required. Hydrostatic journal bearings with pockets are used on servo cylinders' rod ends because they can guarantee the bearing of high loads, low static and dynamic friction and absence of wear. Usually four or six pockets are circumferentially positioned in the bushing and they are continuously fed with fluid through opportunely designed orifices, one for each pocket. Each pocket is surrounded by a bearing land, having the size of the radial clearance between the rod and the cylinder. The fluid coming from the orifices flows through the bearing lands, thus maintaining a good control of the local temperature in the bearings (FIGURE 1). Considerable variations in the design parameters of the hydrostatic journal bearing and in the type of application make not so easy the choice of the optimal design, despite the large number of data that can be found in literature and technical reports. Moreover, the

availability of space, which also can vary from an application to the other, is an important constraint to be considered in the optimization process.

In this paper the classical hydrostatic journal bearing with pockets is studied by means of a numerical procedure that, resolving the Reynolds equation within the gap, allows to calculate the pressure distribution, the drain leakage, the possible radial load arising in the gap, all as function of the geometry of the journal bearing, the manufacturing tolerances and the boundary conditions in the hydraulic cylinder chambers. The fluid considered is a standard mineral oil typically used in fluid power applications, behaving as a Newtonian fluid, in isothermal condition.

The problem of solving the Reynolds equation within the journal bearing gap and considering the effect of the pockets and their contribution to the bearing has already been addressed in literature by many researchers in numerous work: Garg et al. in [7] report a nice review of the work done by researchers during the years (among which, the substantial work of Rowe W.B., who also edited [8], and San Andres L. [9]) focusing in particular on the design problem. They stated that many influence factors were considered in the analysis, as the macro geometry of the journal bearing and pockets, as well as the operating conditions, while still there is a need for more research (both numerical and experimental) work on the influence of thermal effects with non-Newtonian lubricants, surface roughness, and turbulence effect of supply velocity. Another aspect that the authors underline as poorly addressed is the need to design the bearing on the basis of more realistic data since it should operate with good performance over a longer period even after the oil is contaminated. The work presented here aims to be a first step in this direction, since, while considering a Newtonian fluid on one side, wants to incorporate in the analysis some geometrical features related to manufacturing tolerances. A similar analysis has been developed in [10] but here a gas lubricated bearing was considered. In [11] the authors expand their review to different geometries of hydrostatic bearing; focusing on the journal bearing, they stated that the majority of the works from research is dedicated on the study of bearing modelling and dynamic characteristic rather than optimization. If, from one side, it is obvious that the mechanism of bearing a radial load for a hydrostatic journal bearing lays on the ability of the rod to reach an eccentric position, from the other side the influence of the manufacturing tolerances may play a role in influencing this eccentricity. The wide variety of dimensions and applications may require different design optimization and the real journal behaviour as well as its durability depends also on the manufacturing process.

The work presented in this paper concerns the first part of a research activity in which both the behavior of the hydrostatic journal bearing at the rod ends and the piston cylinder gap are going to be modelled, simulated under different operating conditions and designs, and the optimal configuration will be realized with the help on an industrial partner and tested to validate the numerical model. At the end, a virtual design tool developed in OpenModelica enviroment ([12]) will be available for industrial designers to help and guide their work.
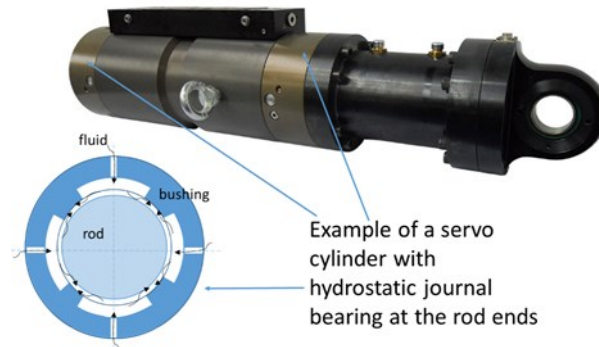

FIGURE 1. A servo cylinder equipped with hydrostatic journal bearing with pockets at the rod ends**.**

THEORETICAL MODEL

As shown in FIGURE 1, the hydrostatic journal bearing is made of an alternation of pockets fed through calibrated orifices and lands between the bushing and the rod, whose radial dimension is defined by the radial clearance between the rod and the bushing. In the following, as typically done in this kind of problems, the analysis is developed considering to unfold the circumferential domain in a plane, shown in FIGURE 2 (a).

The cartesian orthogonal frame of reference used in the schematization is visible in FIGURE 2 , obtained by unrolling the gap surfaces, with the x-axis along the circumferential direction and y-axis coincident with the piston axial direction. In the figure is also shown the reference scheme of an elementary volume.
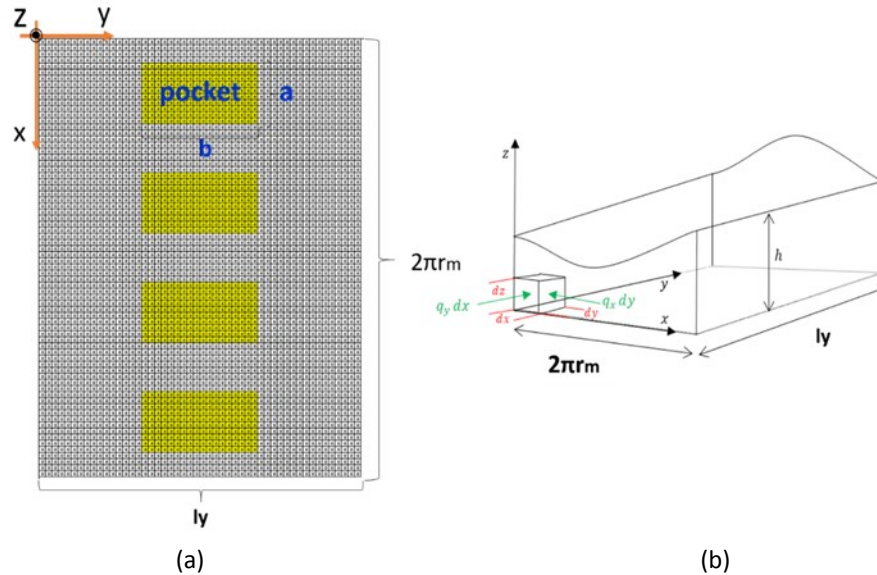

(a)   (b)

FIGURE 2. Frame of reference of the unfolded gap in a 2D (a) and 3D visual (b) together with the frame of reference adopted

To define the domain geometry, the geometrical definition of the height h of the gap is fundamental. The design parameters and manufacturing tolerances are chosen as input data to the problem and the height of the clearance is then considered constant with respect of the time.

The height of the gap between the cylinder and the piston is calculated referring to the case of infinitely long journal bearings (the journal bearing length is several orders of magnitude bigger than the gap height). The FIGURE 3 shows the parameters and correspondent symbols used in the calculation.

This height h is a function of the radial clearance $(r_e\text{-}r_i)$, eccentricity e, roundness rot and conicity c. The eccentricity is to be considered as soon as a radial load is acting on the rod, otherwise no radial reaction is possible from the hydrostatic journal bearing. The roundness manufacturing tolerance rot and the conicity c of the rod are defined in the as in FIGURE 3 (b) and (c) respectively.

(a)   (c)
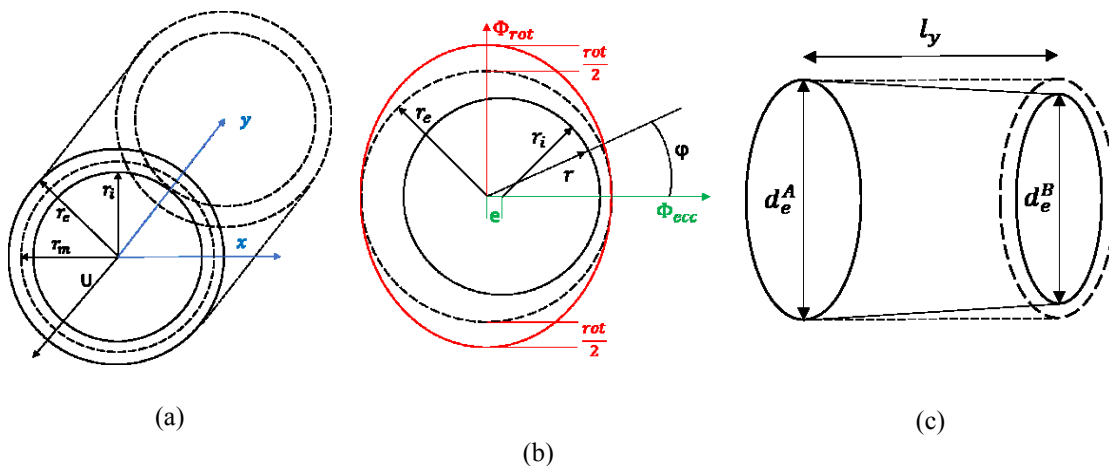
(b)

FIGURE 3. Cylinder schematic representation, with system in balance (a) ,with eccentricity and roundness.(b) and conicity (c)

The cylinder conicity c has been defined, based on the figure, with the equation (1):

$$c = \frac{(d_e^A - d_e^B)}{l_y} \tag{1}$$

The expression for the height of the gap and its derivatives with respect to x and y coordinates are shown in equation (2).

$$h(x,y) = r_e - r_i - e\,\cos\left(\frac{x}{r_m} - \phi_{ecc}\right) + y\frac{c}{2} + \left|\frac{rot}{2}\cos\left(\frac{x}{r_m} - \phi_{rot}\right)\right|$$

$$\frac{dh}{dx}(x,y) = \frac{e}{r_m}\sin\left(\frac{x}{r_m} - \phi_{ecc}\right) + \frac{\frac{rot^2}{2}\left(\phi_{rot} - \frac{x}{r_m}\right)}{2r_m\left|\frac{rot}{2}\cos\left(\phi_{rot} - \frac{x}{r_m}\right)\right|} \tag{2}$$

$$\frac{dh}{dy}(x,y) = \frac{c}{2}$$

The flow rate per unit length contributions q_x and q_y, along the x and y axis are calculated as:

$$q_x = -\frac{1}{12\mu}\frac{\partial p}{\partial x}h^3 \tag{3}$$

$$q_y = -\frac{1}{12\mu}\frac{\partial p}{\partial y}h^3 - U\frac{h}{2}$$

Where p is the pressure, U the fluid velocity of the moving wall in the gap and μ the fluid absolute viscosity.

To calculate the pressure for each pocket (with n_t number of pockets), the flow continuity equation is considered: the flow rate that enters the pocket from the upstream feeding circuit, going across the cylindrical laminar orifice (equation (4)), is equal to the flow leaving the pocket and entering in the gap between the rod and the bushing. The pressure value in the pocket is considered constant in the calculation. Figure 4 represents the connection between the inlet and the pocket through the orifice.
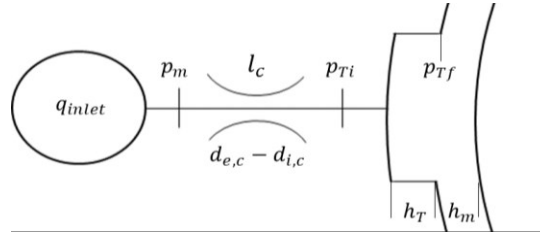

FIGURE 4. Schematization of the laminar orifice on the pocket feeding side

$$\frac{q_{inlet}}{n_t} = \frac{\pi d_{e,c}\left[\frac{(d_{e,c}-d_{i,c})}{2}\right]^3(p_m - p_{Ti})}{12\mu l_c} \tag{4}$$

$$p_{Tf} - p_{Ti} = \frac{\alpha}{2}\rho\left(\frac{q_{inlet}}{n_t}\right)^2\left(\frac{1}{h_T^2} - \frac{1}{h_m^2}\right)$$

In each pocket, the equation of continuity is written as:

$$q_{x,in} - q_{x,out} + q_{y,in} - q_{y,out} = -\frac{q_{inlet}}{n_t} \qquad (5)$$

That equation is numerically solved with the internal iterative method implemented in OpenModelica.
The pressure within the lands between the pockets is calculated using Reynolds equation, considering the following assumptions involved in the analysis summarized below:

- The fluid is incompressible ($\rho = cost$) and Newtonian.
- The Reynold's number is small enough to guarantee laminar flow in the gap.
- The mass forces can be neglected in comparison to viscosity forces.
- The pockets are equally spaced and are sufficiently deep to ensure uniform pressure within their confines
- The elastic deformations of the rod and the bushing are ignored, the axial misalignment of the rod is not considered; the roundness and the conicity (c) of the journal bearing are considered.
- The fluid flow is studied under permanent conditions ($\frac{\partial}{\partial t} = 0$) .

With these basic assumptions of oil lubrication, in order to evaluate the pressure distribution in the clearance between the rod and the bushing, the Reynolds equation, derived from the Navier-Stokes equation, can be written as:

$$\frac{\partial}{\partial x}\left(\frac{\partial p}{\partial x} h^3\right) + \frac{\partial}{\partial y}\left(\frac{\partial p}{\partial y} h^3\right) = 6\mu \left(\omega r_z \frac{\partial h}{\partial x} + U \frac{\partial h}{\partial y}\right) \qquad (6)$$

In the case analyzed the rotational speed ω is equal to zero, as well as the velocity of the moving wall U of the clearance (the piston can move upward and backward inside the cylinder but the case of static piston is here considered).

In this paper the Reynolds equation has been written in the gap, where an opportune mesh was applied, using the finite difference method. A mesh of *NxM* elements is created in the *xy* plane, chosen on the basis of the dimensions of the hydrostatic journal bearing, as the best compromise between accuracy of results (the mesh is chosen after checking different number of elements and stopping the procedure when the deviation on the bearing force between a calculation and the previous one is less than 1%) and computational cost. Giving the boundary conditions, the pressures at the gap ends, a numerical solution is possible for the elements of the rectangular matrix grid using the finite differences method. The results obtained in OpenModelica environment using the internal iterative method have been compared with the results obtained solving the same problem with a home-made code developed in VBA that uses the Gauss-Seidel iteration algorithm.

In a steady state operating condition the rod, subjected to an external radial load, assumes an eccentric position inside the bushing, with a certain eccentricity magnitude (*e*) in direction *Φecc*. This eccentricity determines a radial pressure distribution in the clearance between the shaft and the hydrostatic bearings. In the clearance, with the help of the flow coming from the pockets, is generated a resulting force that had to balance the external forces acting on the piston. The load capacity of the bearings is calculated knowing the value of the pressure distribution.

The total drain leakage is calculated as the sum of the flow axial components (along the y-axis) that escape from the elements of the gap boundaries.

INFLUENCE OF DESIGN AND MANUFACTURING PARAMETERS

In the manufacturing process, the admissible tolerances for each component produced are of fundamental importance, and are directly linked to the cost of manufacturing. In this analysis, the influence of the tolerances, which affect the geometrical definition of the journal bearing, on the bearing force and drain leakage is studied. The following four parameters and their tolerances have been considered:

- radial clearance between the rod and the bearing: ($r_e - r_i$);
- external diameter of the orifice: called d_c, is the diameter of the feeding orifice (depicted in FIGURE 5);
- conicity of the rod: defined in equation 1;
- roundness of the cylinder.

Having defined these parameters, two configurations have been chosen which could be exemplary because of the different sizes: a cylinder of medium size, with a bore of less than 10 cm, called configuration A, and a cylinder about 4 times larger, called configuration B.

TABLE 1. Cylinder dimensions of the chosen configurations, normalized with respect the piston diameter.

Cylinder dimensions	Configuration A	Configuration B
Piston Diameter	D_a	D_b
Rod diameter	$0.75D_a$	$0.78D_b$
Total cylinder displacement	$1.75D_a$	$1.55D_b$
Bushing external radius	$0.37D_a$	$0.39D_b$
Eccentricity	$1.6 \times 10^{-4}D_a$	$6.3 \times 10^{-5}D_b$
Eccentricity Direction	$90°$	$90°$
Roundness	$1.2 \times 10^{-4}D_a$	$3 \times 10^{-5}D_b$
Conicity	$2 \times 10^{-6}D_a$	$6 \times 10^{-7}D_b$
Pocket dimensions, $a = b$	$0.47D_a$	$0.25D_b$
Diameter of the laminar orifice	$0.06D_a$	$0.016D_b$
Radial clearance	$3.2 \times 10^{-4}D_a$	$1.3 \times 10^{-4}D_b$

The pressure at delivery port of the feeding circuit and within the active chamber of the cylinder has been set to 280 [bar] and the pressure at discharge chamber of the cylinder has been set to 1 [bar].

The standard configuration is defined according to the data given by the manufacturer and using the average value of tolerances. The alternative configurations are defined by moving one parameter above and below (four levels) the reference value, within the constraints on the geometrical parameters. The trend of the radial bearing force F and drain leakage q_d is reported, in comparison between the two configurations.
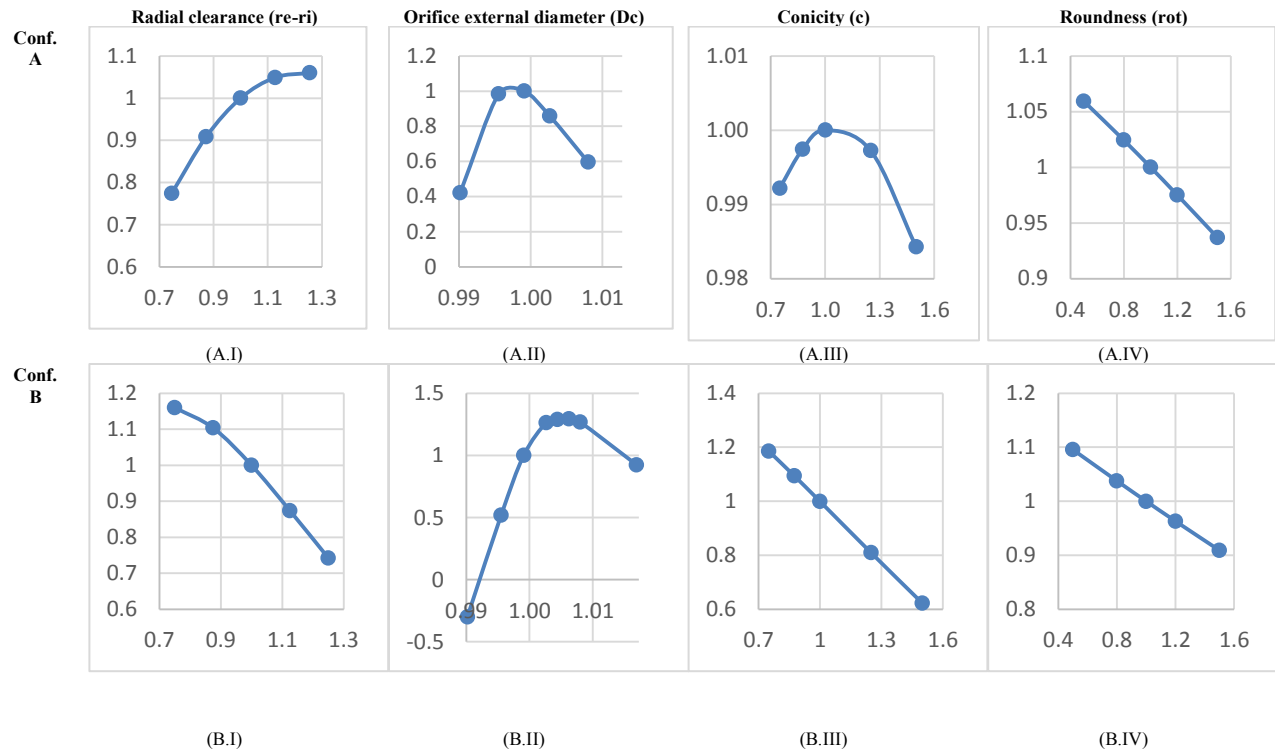
Radial Bearing Force F/F$_{std}$

FIGURE 5 Force results (F/Fstd) for the two configurations analyzed.

The graphs in Figure 5 show the results in terms of radial force, where the values have been normalized according to the standard condition, being able to provide a general overview on the trends; the force is reported as F/F_{std} where F_{std} is the value of the force at the standard configuration and similarly it is done for the drain leakage.

Radial gap:

 Looking at the configuration A (FIGURE 5, A.I) and increasing the radial clearance, it can be seen how the force F/F_{std} tends to reach a higher value, which means the radial load on the cylinder can be higher also; at the opposite, for the bigger cylinder (FIGURE 5, B.I) there would be an improvement on the force if reducing the radial clearance.

The difference between the trends is related to the definition of the standard condition in which have been established the reference values, because these values are linked to the manufacturing tolerances generally used by the industrial partner. An important indication from the results is that in configuration A the manufacturing tolerances on the radial clearance in the journal bearing can be less restrictive, thus helping the journal bearing from the point of view of the radial load bearing capacity. On the other side, configuration B will benefice from a reduction of the radial clearance.

Orifice external diameter:

It is possible to see that there is a value for the diameter of the orifice, which allows obtaining an increased bearing force for both the configurations; in the first case (FIGURE 5, A.II) this point is practically situated at the value chosen as the standard value; for the configuration B this moves towards slightly larger values. It should be emphasized that the optimal point for the d_c can vary in particular with the variation of the radial gap. This is related to the fact that increasing the radial clearance increases the volume the oil has to fill and to maintain a sufficient load bearing capacity the oil flow must also necessarily increase. This is reflected in the need to have a bigger external diameter of the orifice. This is visible, referring only to configuration B, in the FIGURE 6 as the different value of radial gap affects the optimization of the d_c: for a greater gap between the external and internal radius, the optimal external diameter moves towards higher values.

Conicity:

According to results, the conicity has a smaller influence in the smaller configuration (FIGURE 5, A.III); in fact, the same value of conicity in the configuration B where the clearance is longer implies a greater difference on the external diameters taken at the ends of the gap. Looking at configuration B, the bearing radial load is always decreasing when the conicity is higher, as this tolerance is reducing the effect of the eccentric position (that is maintained fixed in these simulations).

Roundness:

The increment of the roundness of the shaft is directly connected with a bigger clearance, as it is shown in the FIGURE 5 (A.IV; B.IV). This is related to the increase in the height of the clearance between rod and bearing and the consequent decrease in pressure.
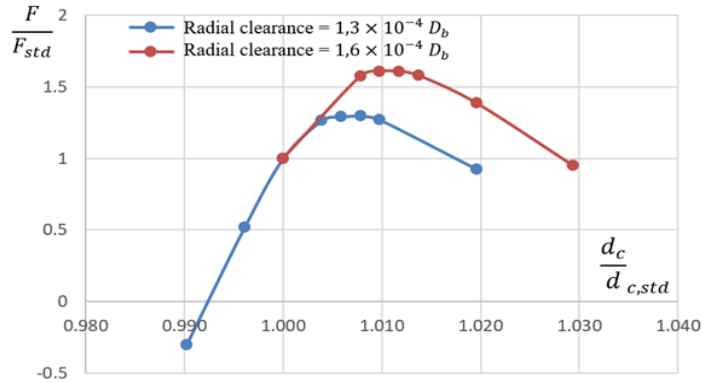
FIGURE 6. Normalized trend of the force related to the orifice diameter, varying the radial clearance value.
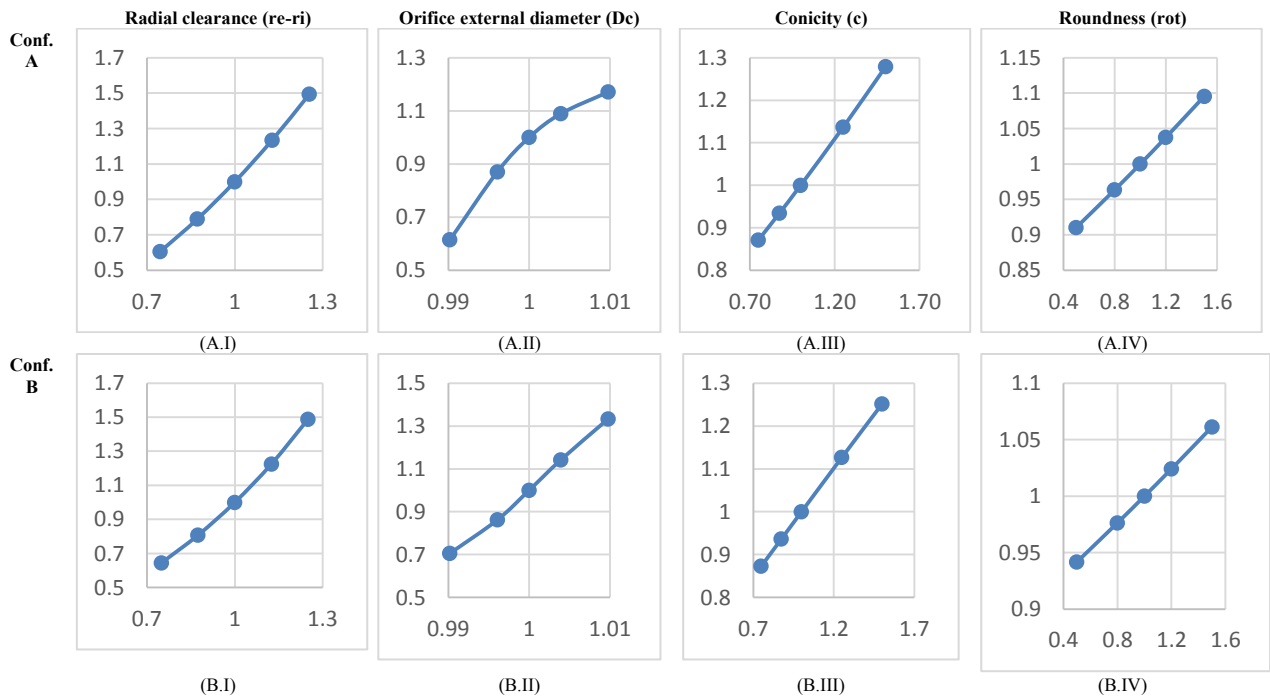
Drain leakage $q_d/q_{d,\,std}$

FIGURE 7. Drain flow $\left(q_d/q_{d,\,std}\right)$ for the two configuration analyzed.

Radial clearance, Conicity, Roundness:

The trend of the drain leakage is always increasing as the parameters related to the cylinder tolerances grow, that are the radial gap, the conicity and the roundness; this is due to the fact that the passage section of the fluid increases and therefore the flow rate will necessarily increase.

Orifice external diameter:

 As regards the external diameter of the orifice (FIGURE 7 A.II,B.II), increasing it will introduce a greater quantity of oil into the bearing and therefore an increase in drainage will occur.

CONCLUSIONS

In this paper the classical hydrostatic journal bearing with pockets is studied by means of a numerical procedure that, resolving the Reynolds equation within the gap, allows to calculate the pressure distribution, the drain leakage, the possible radial load arising in the gap, all as function of the geometry of the journal bearing, the manufacturing tolerances and the boundary conditions in the hydraulic cylinder chambers. The numerical procedure has been developed on OpenModelica environment. The work is part of a larger project that aims to study the lubrication interfaces of a servo cylinder, in particular addressing the influence of the manufacturing tolerances and looking for an optimized configuration which allows reaching the best compromise between obtaining a good load bearing capability of the servo cylinder, a tolerable drain leakage and affordable realization costs for the component.

From the first results regarding the hydrostatic journal bearing at the rod ends of the servo cylinder piston, it can be seen that manufacturing tolerances may play a significant influence on the journal bearing behavior. Therefore an accurate choice of the design parameters, such the radial clearance and the orifice diameter, must be followed by the analysis of the effect of the tolerances which affect them, with the aim of validating the results on the radial bearing force and drain leakage and to look for a possible optimal configuration.

ACKNOWLEDGMENTS

NOMENCLATURE

a, b: pockets dimensions
c: cylinder conicity
d_e^A: external diameter of the greater side (A)
d_e^B: external diameter of the smaller side (B)
$d_{e,c}$: external diameter of the laminar orifice
$d_{i,c}$: internal diameter of the laminar orifice
e: eccentricity magnitude
F : radial bearing force
F_{std} :standard radial bearing force
l_y: bearing length on the axial direction
h: clearance height between piston and cylinder
h_T: height of the pocket
h_m: height of the gap under the pocket
l_c: laminar orifice lenght
l_y: length on the y direction
n_t: number of pockets
p: pressure
p_m: laminar orifice upstream pressure
$p_{T,i}$: laminar orifice downstream pressure and pocket upstream pressure
$p_{T,f}$: pocket downstream pressure
q_d : drain leakage
$q_{d, std}$ drain leakage in the standard configuration
q_x: unitary flow rate , direction x
q_y: unitary flow rate, direction y

q_{inlet}: inlet flow rate in the pockets
$q_{x,in}$: unitary flow rate, along x axis entering the grid cell
$q_{x,out}$: unitary flow rate , along x axis outgoing the grid cell
$q_{y,in}$: unitary flow rate along y axis entering the grid cell
$q_{y,out}$: unitary flow rate along y axis outgoing the grid cell
r_e: external bearing radius
r_i: internal bearing radius
$r_m = \frac{(r_e - r_i)}{2}$: bearing mean radius
rot: roundness magnitude
U: moving wall velocity along y axis
µ fluid dynamic viscosity
ρ: fluid density
ϕ_{ecc}: eccentricity direction
ϕ_{rot}: roundness direction
ω angular speed

REFERENCES

1. Ivantysyn, J. and Ivantysynova, M. (2001). Hydrostatic Pumps and Motors, Principles, Designs, Performance, Modelling, Analysis, Control and Testing. New Delhi.
2. Casoli, P., Bedotti, A., Campanini, F., Pastori, M. (2018) A methodology based on cyclostationary analysis for fault detection of hydraulic axial piston pumps, Energies, 11 (7), art. no. 1874.
3. Rundo M., Altare G. (2018) Lumped Parameter and Three-Dimensional Computational Fluid Dynamics Simulation of a Variable Displacement Vane Pump for Engine Lubrication, ASME J. Fluids Eng. 140(6), 061101-1, 2018. DOI: 10.1115/1.4038761.
4. Corvaglia A., Rundo M. (2018) Comparison of 0D and 3D Hydraulic Models for Axial Piston pumps, Proceedings of the 73th Conference of the Italian Thermal Machines Engineering Association, ATI2018, 12-14 September, 2018, Pisa, Italy. Energy Procedia 148: 114-121, 2018. DOI: 10.1016/j.egypro.2018.08.038. Scopus: 2-s2.0-85056578969.
5. E. Frosina, A. Senatore, D. Buono, K. A. Stelson, F. Wang, B. Mohanty, M. J. Gust, (2015), Vane pump power split trasmission: three dimensional computational fluid dynamic modeling, Proceedings of the ASME/BATH 2015 Symposium on Fluid Power and Motion Control, FPMC2015, Chicago, Illinois, USA, DOI: 10.1115/FPMC2015-9518, Scopus Code: 2-s2.0-84964330332
6. Macor A., Tramontan M. (2007) Hydrostatic hybrid system: System definition and application, International Journal of Fluid Power Volume 8, Issue 2, 2007, Pages 47-62. DOI: 10.1080/14399776.2007.10781276. Codice scopus:2-s2.0-34547626263.
7. Garg, H. , Sharda, H. and Kumar, V. (2006), On the design and development of hybrid journal bearings: a review. Tribotest, 12: 1-19. doi:10.1002/tt.1
8. Vv.Aa. (2012) Handbook of Lubrication and Tribology, Volume II: Theory and Design, Society of Tribologists and Lubrication Engineers, Taylor and Francis, Published July 6, 2012 Reference-1169 Pages-514 ISBN 9781420069082
9. https://rotorlab.tamu.edu/TRIBGROUP/default.htm, accessed last time June the 8th 2019.
10. Stout, K. J. (1985). The Effect of Manufacturing Variations on the Performance of Externally Pressurized Gas-Lubricated Journal Bearings. Proceedings of the Institution of Mechanical Engineers, Part C: Journal of Mechanical Engineering Science, 199(4), 299–309. https://doi.org/10.1243/PIME_PROC_1985_199_127_02
11. Liu, Z., Wang, Y., Cai, L., Zhao, Y., Cheng, Q., & Dong, X. (2017). A review of hydrostatic bearing system: Researches and applications. Advances in Mechanical Engineering. https://doi.org/10.1177/1687814017730536
12. https://openmodelica.org/, last access 8th June 2019